JOURNAL OF PHYSICAL ORGANIC CHEMISTRY, VOL. 9, 561–572 (1996)

AB INITIO MO STUDY OF BENZYLIC CATIONS—1. SOME THEORETICAL PARAMETERS RELATED TO THE RESONANCE DEMAND IN THE YUKAWA–TSUNO EQUATION

KAZUHIDE NAKATA, MIZUE FUJIO,* YOSHIHIRO SAEKI, MASAAKI MISHIMA AND YUHO TSUNO†
Institute for Fundamental Research of Organic Chemistry, Kyushu University, Fukuoka 812, Japan
AND
KICHISUKE NISHIMOTO*‡
Department of Chemistry, Faculty of Science, Osaka City University, Osaka 558, Japan

Structures of 14 kinds of benzylic cations into which are introduced various substituents at benzylic position were optimized by means of the *ab initio* molecular orbital method at the RHF/6-31G* level. The theoretical indices obtained associated with the resonance interaction, such as population, bond order and bond length, were compared with the resonance demand parameter (*r* value) of corresponding solvolysis systems that were given by the Yukawa–Tsuno substituent effect analysis. The *r* value was linearly correlated with the theoretical resonance indices.

INTRODUCTION

Among the structure–reactivity relationships[1] which represent the most fundamental concept in physical organic chemistry, the Hammett equation[2] (equation (1)) regarding the reactions and equilibria of benzene derivatives is most widely used:

$$\log(k/k_0) = \rho\sigma \qquad (1)$$

where k (or K) is the rate (or equilibrium) constant for such a reaction of a ring-substituted derivative and k_0 (or K_0) is the corresponding value for the unsubstituted compound. The intuitive interpretation of this empirical relationship by organic chemists is that substituent effects on reaction rates and equilibria commonly involve polar or resonance interactions of substituents with full or partial ionic charges. The reaction constant ρ then reflects differences in charge, at a functional group or a reaction site, between reactants and products or reactants and transition state.

Despite the broad applicability of the Hammett equation, a clear non-constancy of substituent effects (σ value) has been observed in various reactivity data (rate or equilibrium constants). An important case of such reactions to which the Hammett equation is not applicable is the solvolysis of benzylic derivatives to form carbocation intermediates:

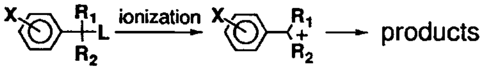

(2)

The Brown equation was proposed in order to correlate the substituent effects on such reactions:[3]

$$\log(k/k_0) = \rho^{+}\sigma^{+} \qquad (3)$$

where σ^{+} is a set of electrophilic substituent constants, which was defined based on the solvolysis rates of *m*- and *p*-substituted α,α-dimethylbenzyl chlorides [R_1, $R_2 = CH_3$, $L = Cl$ in equation (2)]. Important deviations appearing in benzylic solvolyses were reasonably referred to the increased resonance interactions in carbenium ions (intermediates):

(4)

---

* Author for correspondence.

† Present address: Department of Chemistry, Faculty of General Education, Kumamoto University, Kumamoto 860, Japan.

‡ Present address: 1-37-10 Kamotanidai, Sakai City, Osaka 558, Japan.

CCC 0894–3230/96/080561–12

Received 7 February 1996
Revised 23 February 1996

It may be expected that the resonance contribution in the carbenium structure, rather than the structural effects in the neutral initial state, would constitute the important factor in the overall substituent effects on the transition state. The substituent effect would therefore largely reflect the pattern of electron delocalization in the corresponding carbenium ions, and no longer be proportional to the Hammett σ constants. Thus the Brown σ^+ defined by α-cumyl solvolysis should be a good average of the substituent effects on benzylic solvolyses. However, even this σ^+ scale cannot be general for the substituent effects on benzylic reactivities.

The solvolysis of 1-aryl-1-(trifluoromethyl)ethyl tosylates,[4a] carrying a strongly electron-withdrawing α-substituent to generate highly electron-deficient carbocations, clearly failed to give a linear correlation against σ^+. The Brown $\sigma^+\rho^+$ equation was also not applicable to the related solvolyses of the highly electron-deficient carbocation system. Nevertheless, more than 20 solvolysis sets of this class recently reported in the literature[4b] gave good linear free energy relationships against $\log(k/k_0)$ values for this 1-aryl-1-(trifluoromethyl)ethyl system with a correlation coefficient >0·99, and none shows a slope significantly higher than unity. This indicates that a different σ^+ scale, electrophilic substituent constants involving a high resonance demand, would be required for linearly describing the substituent effects in these extremely electron-deficient benzylic systems. Any single $\bar{\sigma}$-scale, apparent substituent parameter scale given by $\bar{\sigma} = \log(k/k_0)/\rho$, would inevitably have limited applicability, and this clearly points to a 'variable response' of the substituents since the extent of electron migration from the substituents to the electron-deficient carbenium centre is largely determined by the intrinsic demand at this position. Thus the theoretical interpretation of substituent parameter scales, σ^0, σ and/or various sets of σ^+ scales as indices of measurement of substituent-ring electronic interactions has received abundant acceptance.

The substituent effects in such systems can be more generally described by the Yukawa–Tsuno (YT) equation:[5]

$$\log(k/k_0) \text{ or } \log(K/K_0) = \rho(\sigma^0 + \mathrm{q}\, r\, \Delta P s_{\mathrm{R}}^{+}) \qquad (5)$$

where σ^0 is the normal substituent constant, which does not involve any additional π-electronic interaction between the substituent and the reaction centre, and $\Delta\bar{\sigma}_{\mathrm{R}}^{+}$ is the resonance substituent constant measuring the capability for π-delocalization of a π-electron donor p-substituent. The r value is a parameter characteristic of a given reaction, measuring the extent of resonance demand, i.e. the degree of resonance interaction between the aryl group and the reaction site in the rate-determining transition state.

The YT equation introduced the concept of varying resonance demand of reactions into the substituent effect analysis. While solvolyses of a series of tertiary α,α-dialkylbenzyl precursors showed linear Brown $\rho^+\sigma^+$ correlations, i.e. $r = 1{\cdot}00$,[4h] the solvolysis of secondary benzylic precursors, e.g. α-phenylethyl chlorides[4d] and α-*tert*-butylbenzyl tosylates,[4c] gives linear correlations with equation (5) with a slightly enhanced r value of 1·1–1·2. The solvolyses of 1-aryl-1-(trifluoromethyl)ethyl tosylates[4a] and 1-aryl-2,2,2-trifluoroethyl tosylates[4b] gave linear YT plots with extremely high r values of 1·39, and 1·51, respectively.

The resonance demand of a carbenium ion may be reduced effectively by reduced coplanarity between the reaction centre and the phenyl ring. A well known example is the solvolysis of α,α-di-*tert*-butylbenzyl p-nitrobenzoates,[4j] which affords an excellent linear YT correlation with $r = 0{\cdot}26$, a value comparable to the r value for the Hammett σ scale. The solvolysis of 4-methylbenzobicyclo[2.2.2]octen-1-yl triflates[4k] would be an excellent model of such a system where the carbocation orbital developed at the bridgehead of the bicyclic skeleton is rigidly orthogonal to the benzo π orbital. This solvolysis was found to give $r = 0{\cdot}0$, being the lowest limit of exalted π delocalization.

There is clearly a wide range of resonance demand r values for a series of benzylic solvolyses (in Table 1), from $r = 0$ for unexalted resonance system to a temporary ceiling value of $r = 1{\cdot}5$, and $r = 1{\cdot}00$ given for the Brown σ^+ scale does not reflect any particular situation of benzylic resonance exaltation but is merely a point in the r scale of resonance demand.

The most effective approach to substituent effects in various solvolyses is by investigating the behaviour of carbocations in the gas phase.[6] We have shown that the YT equation is applicable to the gas-phase substituent effects on the intrinsic stabilities of various benzylic cations in exactly the same manner as applies to the solution phase. The r value significantly increases as the parent carbocation becomes less stable, while the ρ value remains constant for a series of benzylic carbocations.[6] Further, it is surprising that the r values for the gas-phase stabilities of the cations have magnitudes identical with those of the corresponding benzylic $S_{\mathrm{N}}1$ solvolyses (Table 1). From this identity, the varying resonance demand r in solvolysis should be an essential feature of the incipient carbocation intermediate and also of the solvolysis transition state. The transition state of $S_{\mathrm{N}}1$ solvolysis can be modelled most reasonably by the structures of cations.

Whereas the advanced theory at present cannot predict unambiguously the structures of the transition state molecules and their characteristic quantities of $S_{\mathrm{N}}1$ reactions, the structures and such quantities of the ground state molecules of benzylic cations can be quantitatively calculated by the *ab initio* method. The value of r, reflecting the π-delocalization within the cationic species, appears to remain essentially the same in solution as in the gas phase, and the degree of charge delocalization in the transition state of the solvolytic

Table 1. Summary of r values in solvolyses and gas phase for some benzylic systems

R_1,R_2[a]	$r_{\text{sol.}}$[b]	r_{gas}[c]
CF_3,H	1·51[d]	1·53[e]
CF_3,Me	1·39[f]	1·40[g]
H,H	1·28[h]	1·29[i]
Me,H	1·15[j]	1·14[k]
t-Bu,H	1·09[l]	
Me,Me	1·00[m]	1·00[n]
Et,Me	1·04[o]	1·01[p]
Et,Et	1·02[q]	0·98[q]
i-Pr,*i*-Pr	1·01[o]	
t-Bu,Me	0·91[r]	0·86[s]
t-Bu,*neo*-Pen	0·78[q]	0·81[q]
t-Bu,*i*-Pr	0·71[q]	
t-Bu,*t*-Bu	0·26[t]	
Benzobicyclo	0·00[u]	

[a] R_1 and R_2 are substituents at the α position.
[b] r Values given in the YT analysis of the solvolyses.
[c] r Values given in the YT analysis of the gas-phase stabilities.
[d] Ref. 4b.
[e] Ref. 6a.
[f] Ref. 4a.
[g] Ref. 6b.
[h] Ref. 4c.
[i] Ref. 6c.
[j] Ref. 4d.
[k] Ref. 6d.
[l] Ref. 4e.
[m] Definition, Ref. 3.
[n] Ref. 6f.
[o] Ref. 4h.
[p] Ref. 6e.
[q] Unpublished results in this laboratory.
[r] Ref. 4i.
[s] Ref. 6g.
[t] Ref. 4j.
[u] Ref. 4k.

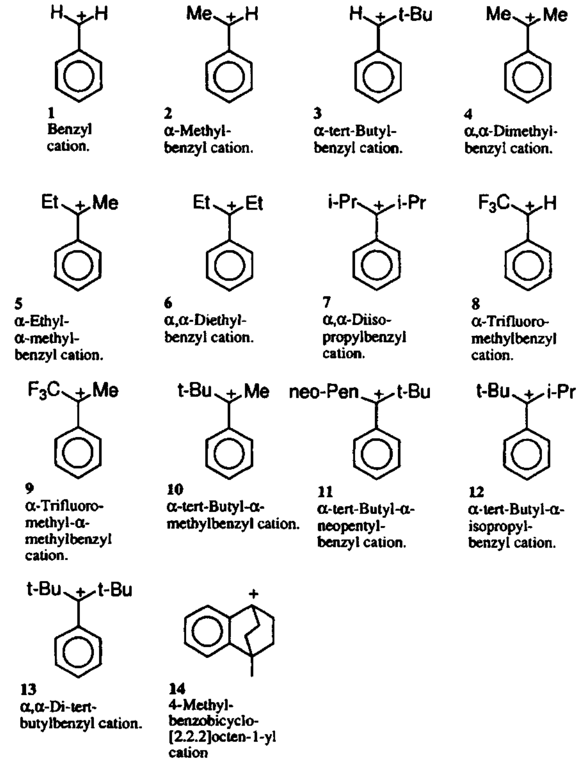

1 Benzyl cation.
2 α-Methylbenzyl cation.
3 α-tert-Butylbenzyl cation.
4 α,α-Dimethylbenzyl cation.
5 α-Ethyl-α-methylbenzyl cation.
6 α,α-Diethylbenzyl cation.
7 α,α-Diisopropylbenzyl cation.
8 α-Trifluoromethylbenzyl cation.
9 α-Trifluoromethyl-α-methylbenzyl cation.
10 α-tert-Butyl-α-methylbenzyl cation.
11 α-tert-Butyl-α-neopentylbenzyl cation.
12 α-tert-Butyl-α-isopropylbenzyl cation.
13 α,α-Di-tert-butylbenzyl cation.
14 4-Methylbenzobicyclo[2.2.2]octen-1-yl cation

Figure 1. Benzylic cations studied (**1**–**14**)

ionization should also resemble that in the carbocation intermediate. Moreover, the r value is directly related to the intrinsic stability of the parent cation. Thus, *ab initio* MO calculations can be used to find the underlying relationship between quantum chemical quantities and experimental r values. The relationship between theoretical indices and the empirical r values for a series of benzylic systems corroborates the characterization of the resonance demand parameter r in the YT equation as a parameter reflecting the degree of π delocalization interaction between the aryl group and the reaction site.

METHOD

Ab initio LCAO–MO calculations[7] were carried out for the α-substituted benzyl cations shown in Figure 1.

Details of the optimized structures with respect to the steric hindrance of cations **10**–**14** will be reported in a subsequent paper. All calculations were performed on an IBM RS/6000 computer with the Gaussian-92 suite of programs.[8] Geometries were optimized completely by the gradient procedure at C_1 symmetry. The closed-shell restricted Hartree–Fock calculation with STO-3G, 3–21G and 6–31G* basis sets was applied to find stationary points on the potential energy surface (PES). At the RHF/6–31G* level all optimized structures were checked by the analysis of harmonic vibrational frequencies obtained from diagonalization of force constant matrices. To improve the calculated energies, electron-correlation contributions were estimated by Møller–Plesset perturbation theory;[9] single-point MP2 calculations were carried out at the 6–31G* basis set using the frozen-core approximation. The relative final energies were corrected for RHF/6–31G* zero-point energy (ZPE) differences scaled by a factor of 0·9.[10] In order to discuss quantitatively the relationship between the r value in the YT equation and populations of electrons at atomic centres, Mulliken population analysis (MPA)[11] was carried out for benzylic cations at the RHF/6–31G* level. Wiberg bond orders in natural bonding orbital (NBO)[12] analysis were also calculated to discuss the origin of the r value. For α-methylbenzyl cations (**2a**–**c**) whose conformations are α-methyl rotamers of one another, calculations were extended to MP2(FU)/6-31G* optimization to estimate the effect of electron correlation on the structure.

RESULTS AND DISCUSSION

Energies and geometries

The numbering of atoms is given in Figure 2. The optimized structures of benzylic cations at the RHF/6-31G* level are shown in Figures 3-6, and their selected geometric parameters are summarized in Tables 2-5. The ϕ values in these tables are the dihedral angles of the $R_1C_7R_2$ plane with respect to the aromatic plane. Total energies are listed in Table 6. Calculated dihedral angles of $\angle R_1C_7C_1R_2$, $\angle C_2C_1C_7C_6$, $\angle C_1C_2C_3C_4$, $\angle C_2C_3C_4C_5$, $\angle C_3C_4C_5C_6$, $\angle C_4C_5C_6C_1$, $\angle C_5C_6C_1C_2$ and $\angle C_6C_1C_2C_3$ for all benzylic cations are less than 3·0°, indicating that phenyl rings and $R_1C_7R_2C_1$ planes actually have coplanar frameworks, respectively. The effects of α-substituents (R_1,R_2) on the electronic structure of the cations and on the change of dihedral angle ϕ can be considered to be real factors to determine the degree of resonance interaction for these benzylic cations, which are reflected in the changes in charge densities and bond orders at the aromatic moiety. Optimized geometries of the individual benzylic cation are discussed below.

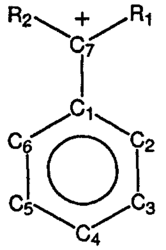

Figure 2. Numbering of atoms for α-substituted benzylic cations

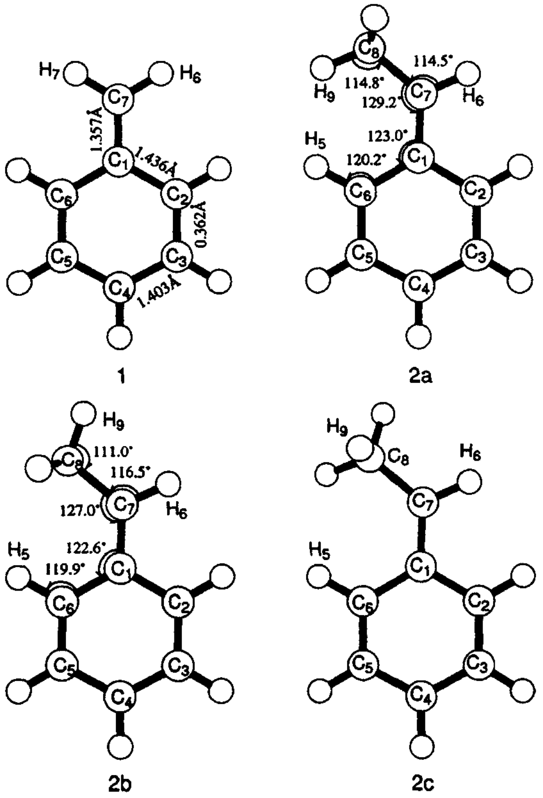

Figure 3. RHF/6-31G* optimized structures of **1**-**2c**

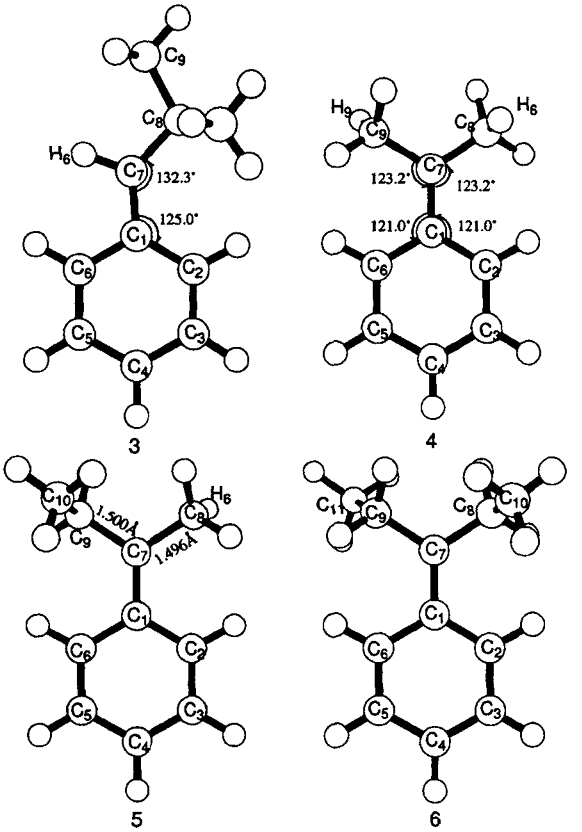

Figure 4. RHF/6-31G* optimized structures of **3**-**6**

Benzyl cation (**1**)

For the benzyl cation, some optimized structures obtained by the *ab initio* MO method have been

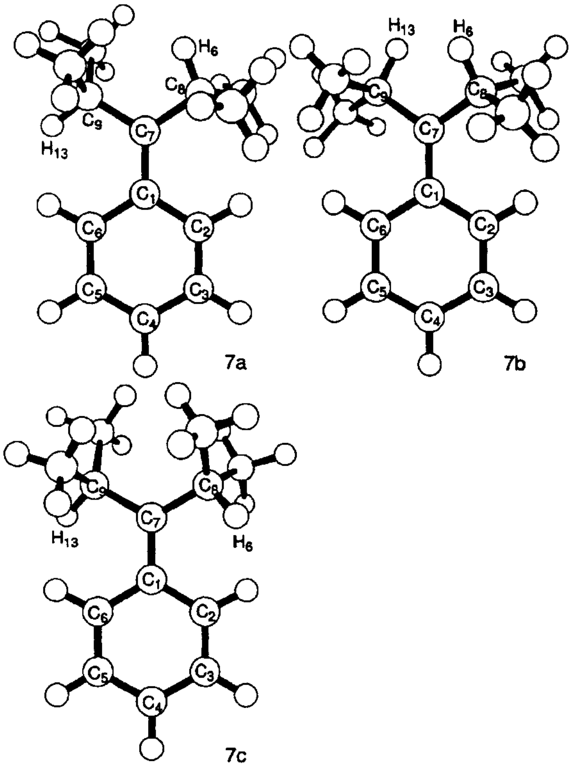

Figure 5. RHF/6-31G* optimized structures of **7a–c**

Table 2. Selected geometric parameters[a] of **1–2c** optimized at the RHF/6-31G* level

	Cation			
	Benzyl	α-Methylbenzyl		
	(**1**)	(**2a**)	(**2b**)	(**2c**)
C_1—C_2	1·436	1·428	1·426	1·427
C_2—C_3	1·362	1·368	1·369	1·368
C_3—C_4	1·403	1·396	1·395	1·395
C_4—C_5	1·403	1·402	1·403	1·402
C_5—C_6	1·362	1·364	1·363	1·364
C_6—C_1	1·436	1·429	1·429	1·429
C_1—C_7	1·357	1·378	1·378	1·378
C_7—R_1[b]	1·075	1·078	1·077	1·077
C_7—R_2[b]	1·075	1·481	1·490	1·484
C_7—C_1—C_2	120·4	118·0	118·5	118·2
C_7—C_1—C_6	120·4	123·0	122·6	122·9
C_1—C_7—R_1[b]	121·7	116·3	116·4	116·3
C_1—C_7—R_2[b]	121·7	129·2	127·0	128·3
ϕ[c]	0	0	0	1

[a] Distances in Å and angles in degrees.

[b] R_1 and R_2 correspond to right- and left-hand side atoms, respectively, bonded to C_7 shown in Figure 3. The numbering of atoms is given in Figure 2.

[c] Mean dihedral angles $\angle R_1C_7C_1C_6$ and $\angle R_2C_7C_1C_6$.

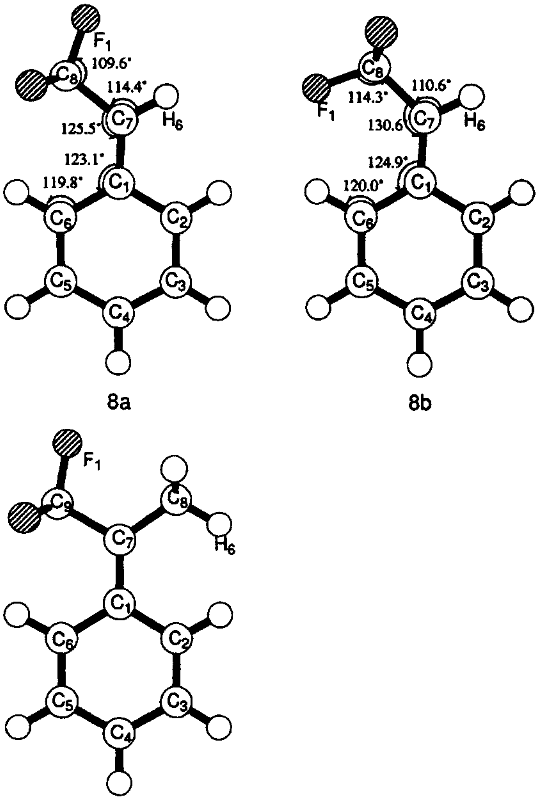

Figure 6. RHF/6-31G* optimized structures of **8a–9**

reported.[13,14] The optimized structure with RHF/6-31G* (Figure 3) is essentially the same as that with RHF/3-21G.[14] The C_1—C_2 (1·436 Å) and C_3—C_4 (1·403 Å) bonds are longer and C_2—C_3 (1·362 Å) is shorter than the C—C bond of benzene (1·39 Å). The contributions of charge-transferred structures shown in Figure 7 form a partial quinoid structure of the benzene ring. This is in accord with the general prediction of resonance theory for charge delocalized benzylic cations, and the same is true for other species.

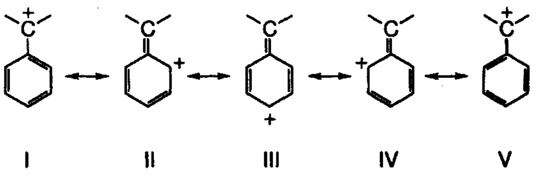

Figure 7. Resonance structures of benzylic cations

Table 3. Selected geometric parameters[a] of **3**–**6** optimized at the RHF/6–31G* level

	Cation			
	α-*tert*-Butylbenzyl (**3**)	α,α-Dimethylbenzyl (**4**)	α-Ethyl-α-methylbenzyl (**5**)	α,α-Diethylbenzyl (**6**)
C_1—C_2	1·429	1·423	1·422	1·422
C_2—C_3	1·364	1·369	1·370	1·371
C_3—C_4	1·402	1·395	1·394	1·394
C_4—C_5	1·393	1·395	1·394	1·394
C_5—C_6	1·370	1·369	1·370	1·371
C_6—C_1	1·427	1·424	1·422	1·422
C_1—C_7	1·386	1·404	1·407	1·410
C_7—R_1[b]	1·511	1·496	1·496	1·500
C_7—R_2[b]	1·078	1·495	1·500	1·500
C_7—C_1—C_2	125·0	121·0	121·0	121·0
C_7—C_1—C_6	116·7	121·0	121·0	121·0
C_1—C_7—R_1[b]	132·3	123·2	122·5	122·8
C_1—C_7—R_2[b]	113·6	123·2	123·0	122·8
ϕ[c]	0	5	3	0

[a,c] See footnotes a and c in Table 2.

[b] R_1 and R_2 correspond to right- and left-hand side atoms, respectively, bonded to C_7 shown in Figure 4. The numbering of atoms is given in Figure 2.

Table 4. Selected geometric parameters[a] of **7a**–**c** optimized at the RHF/6–31G* level

	Cation		
	α,α-Diisopropylbenzyl		
	(**7a**)	(**7b**)	(**7c**)
C_1—C_2	1·423	1·419	1·422
C_2—C_3	1·371	1·372	1·372
C_3—C_4	1·393	1·392	1·392
C_4—C_5	1·392	1·392	1·392
C_5—C_6	1·371	1·372	1·372
C_6—C_1	1·424	1·419	1·422
C_1—C_7	1·418	1·419	1·425
C_7—R_1[b]	1·522	1·517	1·518
C_7—R_2[b]	1·513	1·517	1·518
C_7—C_1—C_2	121·6	121·3	121·5
C_7—C_1—C_6	121·5	121·3	121·5
C_1—C_7—R_1[b]	123·9	123·8	119·0
C_1—C_7—R_2[b]	121·3	123·7	119·0
ϕ[c]	10	21	14

[a,c] See footnotes a and c in Table 2.

[b] R_1 and R_2 correspond to right- and left-hand side atoms, respectively, bonded to C_7 shown in Figure 5. The numbering of atoms is given in Figure 2.

α-Methylbenzyl cation (**2**)

The α-methylbenzyl cation has been converged into two stationary conformations: **2a** ($\angle H_9C_8C_7C_1 = 0°$) and **2b** ($\angle H_9C_8C_7C_1 = 180°$) as shown in Figure 3. Structure **2a** is more stable by 1·14 kcal mol^{-1} (1 kcal = 4·184 kJ) than **2b** at the MP2/6–31G*//RHF/6–31G* + ZPE (scaled 0·9) level. Surprisingly, frequency calculation shows that structure **2b** is the transition state having one imaginary frequency. This result is very strange, because, for example, for the internal rotation of ethane molecule the conformation corresponding to **2a** is the transition-state structure and that to **2b** is the most stable structure. The normal mode associated with this imaginary frequency indicates that rotation of the methyl group leads to the lower energy structure. This strange problem has not yet been solved. When we optimize **2c** with a 90° fixed dihedral angle ($\angle H_9C_8C_7C_1 = 90°$), then we obtain a structure which is less stable by 0·54 kcal mol^{-1} (comparable to kT) than **2a**. When this constraint is removed, the geometry is converged to **2a**. Hence **2a** is considered to be the global minimum at the RHF/6–31G* level. Hartree–Fock theory cannot estimate the electron correlation effect which is exerted on the structure. For example, the bridged form for the ethyl cation is the global minimum at levels more than MP2, and further the open cation is predominant at the RHF/6–31G* or RHF/3–21G level.[15] Therefore, the geometry optimization of **2a**–**c** has been extended to the MP2(FU)/6–31G* level. The angle $\angle H_9C_8C_7$ was to be 107·4°, which is almost the same as but slightly less than the normal tetrahedral angle. Structure **2a** was more stable than **2c** by 0·56 kcal mol^{-1} at the MP2(FU)/6–31G* level. Hence the alignment of the C—H bond with the vacant 2pπ-orbital is not a predominant factor to stabilize the cation **2**. This might be attributed to the larger charge delocalization to the aromatic moiety (+0·56 for **2a**-**2c**) in these benzylic cations. This is in contrast to charge-localized alkyl cation systems.[15–17] Structure **2b** is less stable than **2a** by 1·26 kcal mol^{-1} at

Table 5. Selected geometric parameters[a] of **8a**–**9** optimized at the RHF/6–31G* level

	Cation		
	α-Trifluoromethylbenzyl (**8a**)	α-Trifluoromethylbenzyl (**8b**)	α-Trifluoromethyl-α-methylbenzyl (**9**)
C_1—C_2	1·443	1·446	1·438
C_2—C_3	1·360	1·360	1·362
C_3—C_4	1·403	1·403	1·400
C_4—C_5	1·406	1·405	1·398
C_5—C_6	1·359	1·359	1·364
C_6—C_1	1·445	1·446	1·440
C_1—C_7	1·353	1·354	1·379
C_7—R_1[b]	1·076	1·076	1·490
C_7—R_2[b]	1·523	1·518	1·543
C_7—C_1—C_2	118·2	116·7	120·8
C_7—C_1—C_6	123·1	124·9	121·8
C_1—C_7—R_1[b]	120·2	118·8	126·5
C_1—C_7—R_2[b]	125·5	130·6	120·0
ϕ[c]	0	0	0

[a,c] See footnotes a and c in Table 2.

[b] R_1 and R_2 correspond to right- and left-hand side atoms, respectively, bonded to C_7 shown in Figure 6. The numbering of atoms is given in Figure 2.

Table 6. Total energies of substituted benzyl cations

	Calculated total energy (−au)				
Cation[a]	RHF/STO-3G	RHF/3–21G	RHF/6–31G*	MP2/6–31G*//RHF/6–31G*	ZPE[b]
1	265·654106	267·380453	268·886732	269·740682	−0·125692(0)
2a	304·252772	306·215505	307·937589	308·925073	−0·155503(0)
2b	304·251557	306·214174	307·935767	308·923118	−0·155213(1)
2c	304·252162	306·214852	307·936726	308·924201	−0·155346(0)[c]
3	419·990743	422·675104	425·037309	426·426977	−0·246438(0)
4	342·844810	345·044469	346·981039	348·103622	−0·185231(0)
5	381·427386	383·866601	386·016827	387·271753	−0·216495(0)
6	420·009129	422·688605	425·052517	426·440163	−0·247754(0)
7a	497·159483	500·319048	503·110505	504·769321	−0·308218(0)
7b	497·155158	500·314478	503·106549	504·766081	−0·307844(0)
7c	497·156050	500·314792	503·106689	504·765623	−0·308815(0)
8a	596·606702	601·162418	604·485146	605·972559	−0·131997(0)
8b	596·605947	601·162416	604·484959	605·971916	−0·132222(0)
9	635·202371	639·997766	643·531254	645·156203	−0·161853(0)

[a] Numbers as in Figure 1.

[b] Zero-point energies (uncorrected) at the RHF/6–31G* level. Values in parentheses are the number of imaginary frequencies in the frequency calculation.

the same level (MP2/6–31G*) of calculations. At all levels of theory and basis sets, a hydrogen-bridged structure has not been found as a stationary point, and **2a** is the most stable structure.

α-tert-Butylbenzyl cation (**3**)

Coplanarity between the $R_1C_7R_2$ plane and the benzene ring is retained ($\phi = 0°$) for all basis sets, although the large steric strain between the *t*-Bu group and the benzene ring results in $\angle C_7C_1C_2 = 125{\cdot}0°$ and $\angle C_1C_7R_1 = 132{\cdot}3°$ at the RHF/6–31G* level (Figure 4). The resonance stabilization overwhelms steric hindrance to make the cation coplanar in this system.

α,α-Dimethylbenzyl cation (**4**)

For **4**, the geometry is slightly basis set dependent; $\phi = 0°$ at the RHF/STO–3G, while $\phi = 5°$ at the RHF/6–31G* (Figure 4) and RHF/3–21G levels. Angles

$\angle C_9C_7C_1$, $\angle C_8C_7C_1$, $\angle C_6C_1C_7$ and $\angle C_2C_1C_7$ are larger by 2·1° on average than the normal angle of an sp^2 carbon. It can be concluded that steric strain exists even in this simplest tertiary benzylic cation in order to attain full resonance stabilization.

α-Ethyl-α-methylbenzyl cation (**5**)

One energy minimum structure **5** (Figure 4), was obtained with all basis sets. There is little difference in the geometry of the parent system on changing the α-substituent from Me to Et.

α,α-Diethylbenzyl cation (**6**)

The geometry was converged to C_2 symmetry (Figure 4) with all basis sets. Some steric strain exists as in cations **4** and **5**.

α,α-Diisopropylbenzyl cation (**7**)

Three minimum energy structures were obtained for all basis sets (Figure 5). This can be explained by the combination of configuration of isopropyl groups. At the final level calculation [MP2/6–31G*//RHF/6–31G* + ZPE (scaled 0·9)], the energy differences of these three species are small; **7a** ($\phi = 10°$) is more stable than **7b** by 1·8 kcal mol^{-1} and **7b** ($\phi = 21°$) is more stable than **7c** ($\phi = 14°$) by 0·8 kcal mol^{-1}. The smallest dihedral angle ϕ (**7a**) is the most preferred conformation. Hence in this cation the resonance stabilization also overwhelms the steric hindrance.

α-Trifluoromethylbenzyl cation (**8**)

Two minimum structures, **8a** ($\angle F_1C_8C_7C_1 = 180°$) and **8b** ($\angle F_1C_8C_7C_1 = 0°$), were found at the RHF/6–31G* level as shown in Figure 6. The energy difference between these two conformations is very small, in contrast the α-methylbenzyl cation (**2**); **8a** is more stable than **8b** by only 0·1 kcal mol^{-1} (less than *kT*). This means that free rotation is expected in this molecule at room temperature. An energy minimum structure at $\angle F_1C_8C_7C_1 = 90°$ does not exist. Even at our final level of calculation [MP2/6–31G*//RHF/6–31G* + ZPE (scaled 0·9)], the energy difference is also small: **8a** is more stable than **8b** by only 0·5 kcal mol^{-1} (less than *kT*).

α-Trifluoromethyl-α-methylbenzyl cation (**9**)

The configuration of two α-substituents is a combination of those for the CF_3 group in **8a** and the CH_3 group in **2a** as shown in Figure 6. Another conformation in which $\angle F_1C_9C_7C_1 = 0°$ and $\angle H_6C_8C_7C_1 = 180°$ was not calculated.

Theoretical parameters associated with the resonance interaction

As is easily predicted from Figure 7, the resonance interaction in the π-conjugated system leads to changes in charge density, bond order and bond length. The Hückel MO (HMO) method is a very useful tool for the qualitative discussion of the reactivity of π-conjugated systems. For example, the Woodward–Hoffmann rule[18] for stereospecific reactions was developed on the basis of the HMO method. In HMO theory, the effect of a substituent on the change in delocalization energy, $\Delta\Delta E_{\mathrm{del}}$, which measures the change in the degree of resonance interaction, can be expressed as follows:

$$\Delta\Delta E_{\mathrm{del}} = \Sigma\Delta q_\mu \alpha_\mu + \Sigma\Sigma\Delta p_{\mu\nu}\beta_{\mu\nu} \tag{6}$$

where Δq_μ and $\Delta p_{\mu\nu}$ are the changes in charge density at the μth atom and that of bond order associated with the $\mu-\nu$ bond, respectively, and α_μ and $\beta_{\mu\nu}$ are usual Coulombic and resonance integrals, respectively. Further, it has been reported that there is a linear relationship between bond order and bond length.[19] The $C(sp^2)$—$C(sp^2)$ bond length, $r_{\mu\nu}$, is given by

$$r_{\mu\nu}/\text{Å} = 1{\cdot}517 - 0{\cdot}180p_{\mu\nu} \tag{7}$$

where $p_{\mu\nu}$ is the π bond order associated with the $\mu-\nu$ bond. Thus the calculated bond length, charge density and bond order would be the theoretical parameters associated with the degree of resonance interaction. We shall examine the relationship between the resonance demand *r* and theoretical parameters associated with the degree of resonance interaction below.

Charge vs *r* value

In organic chemistry, charge distribution is very useful tool to predict reactivities. Resonance stabilization of conjugated benzylic cations leads to their charge delocalizations. Hence the charge distribution should be directly related to the *r* value. Atomic charges on the carbons of benzylic cations, calculated by Mulliken population analysis (MPA), are summarized in Table 7. Averaged values are used for atomic charges on *ortho* $[(C_2 + C_6)/2]$ and *meta* $[(C_3 + C_5)/2]$ positions. The charge on a hydrogen is summed into that on the carbon atom (group charges). Therefore, the Mulliken charge population on the C_1 atom having no hydrogen should not be compared directly with those on other carbons. For this reason, the charges on the *ortho* carbon for **14** also cannot be compared with those for other species. The atomic charges (given by MPA) on *ortho*, *meta* and *para*-positions for benzylic cations are plotted against the *r* values in Figure 8. In Figure 8 for most cations, charges at atomic positions are related linearly to the *r* values. The deviation is significant for the cation **14**, which involves extremely high inner strain. Apart from this, there are fairly good linear correlations

Table 7. Atomic charges given by Mulliken population analysis for benzylic cations (RHF/6–31G*)

Cation[a]	Charge[b] (RHF/6–31G*)			
	C_1	*Ortho*[c]	*Meta*[d]	*Para*[e]
1	−0·024	0·189	0·051	0·213
2a	−0·050	0·164	0·046	0·190
3	−0·040	0·154	0·041	0·182
4	−0·068	0·140	0·043	0·171
5	−0·066	0·137	0·041	0·166
6	−0·066	0·135	0·039	0·163
7a	−0·076	0·133	0·034	0·160
8a	−0·030	0·211	0·053	0·233
9	−0·074	0·191	0·046	0·211
10	−0·074	0·123	0·039	0·153
11	−0·078	0·110	0·036	0·137
12	−0·088	0·054	0·053	0·077
13	−0·053	0·074	0·037	0·073
14	−0·081	0·043	0·069	0·078

[a] Numbers as in Figure 1.
[b] Atomic charges on each position with hydrogens summed into heavy atoms given by MPA.
[c] Average atomic charge of C_2 and C6.
[d] Average atomic charge of C_3 and C_5.
[e] Atomic charge of C_4.

against *r* values for the charge populations at the *ortho* (correlation coefficient $R = 0{\cdot}96$) and *para* positions ($R = 0{\cdot}97$), but no significant change in the charge distribution at the *meta* position. As the *r* value increases, the charge at the *para* position increases significantly to +0·2 at $r = 1{\cdot}5$ in the correlation, whereas the charge at the *meta* position changes much less (slope = 0). This trend of charge delocalization for benzylic cations is consistent with the varying degree of resonance stabilization.

The Mulliken charge distribution at the respective atomic positions should be regarded as reflecting the demand of the α-cationic centre of benzylic carbocations for the π-electron delocalization from those atomic positions and should be directly related to the *r* value. In Figure 8, the charges at various atomic positions for a series of benzylic cations are linearly related to the *r* values. There are linear correlations of the charge populations at the respective carbon atoms with the *r* value, but there is no significant change in the population at the *meta* carbon atom.

The sum of atomic charges on the phenyl ring should be a probe measuring the conjugative interaction between C_7 and the aromatic moiety. Charges on the aromatic moiety of each benzylic cation are plotted against the *r* values in Figure 9. A linear correlation was found ($R = 0{\cdot}93$) apart from cation **14**. The total charges on the aromatic moiety increase with increase in *r*. This suggests that charge delocalization to the aromatic moiety is the intrinsic factor determining the *r* value.

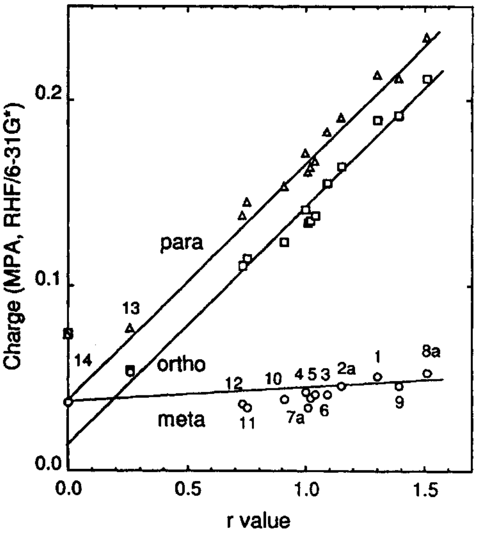

Figure 8. Mulliken population on *o*-, *m*- and *p*-positions of phenyl ring (RHF/6–31G*) vs *r* values for benzylic cations. Numbers as in Figure 1.

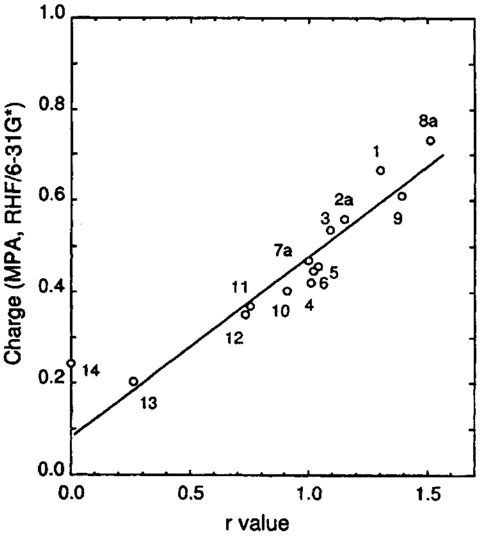

Figure 9. Sum of Mulliken population on phenyl ring (RHF/6–31G*) vs *r* values for benzylic cations. Numbers as in Figure 1

Wiberg bond orders vs *r* value

The contributions of resonance structures **II**, **III** and **IV** shown in Figure 7 become more important with increase in resonance interaction between the benzylic $2p\pi$ orbital and the benzene π system. This brings about changes in bond order of C_1—C_7 and averaged bond orders of C_1—C_2 and C_6—C_1, C_2—C_3 and C_5—C_6, and C_3—C_4 and C_4—C_5, which are summarized in Table 8. The Wiberg bond order[20] is plotted against the *r* value in Figure 10. The C_1—C_7 bond order converges to 1·0 at $r=0$, which corresponds to a pure single bond shown in structures **I** and **V** in Figure 7. The Wiberg index for the C_1—C_7 bond increases linearly with the *r* value, indicating an increase in the contribution of structures **II**, **III** and **IV** ($R=0{\cdot}97$). This tendency reveals that the *r* value shows the degree of overlap between the benzylic pπ orbital and the benzene π system. The bond orders of C_1—C_2 ($R=0{\cdot}97$), C_2—C_3 ($R=0{\cdot}98$) and C_3—C_4 ($R=0{\cdot}98$) also change linearly, reflecting the relative importance of the contribution of canonical structures (**I**–**V**) in Figure 7. All these Wiberg indices converge to 1·4 at $r=0$. As *r* increases, the Wiberg indices for C_2—C_3 increase but those for C_1—C_2 and C_3—C_4 decrease, indicating the increase in the contribution of the resonance structures (**II**–**IV**). All these behaviours are consistent with the prediction of resonance theory, indicating an increasing resonance interaction between C_7 and the aromatic moiety as the *r* value increases.

Table 8. Wiberg bond orders from NBO analysis calculated at the RHF/5-31G* level for benzylic cations

Cation[a]	Wiberg bond order[b]			
	C_1—C_7[c]	C_1—C_2[d]	C_2—C_3[e]	C_3—C_4[f]
1	1·584	1·158	1·567	1·343
2a	1·465	1·193	1·543	1·361
3	1·447	1·203	1·536	1·366
4	1·363	1·225	1·524	1·375
5	1·352	1·231	1·521	1·377
6	1·343	1·235	1·518	1·379
7a	1·338	1·239	1·515	1·381
8a	1·622	1·134	1·585	1·329
9	1·506	1·166	1·561	1·347
10	1·306	1·253	1·507	1·386
11	1·249	1·279	1·492	1·396
12	1·049	1·370	1·444	1·428
13	1·017	1·371	1·422	1·433
14	1·017	1·386	1·435	1·433

[a] Numbers as in Figure 1.
[b] Ref. 19.
[c] Wiberg bond orders of C_1—C_7 bond.
[d] Average of C_1—C_2 and C_6—C_1 bonds.
[e] Average of C_2—C_3 and C_5—C_6 bonds.
[f] Average of C_3—C_4 and C_4—C_5 bonds.

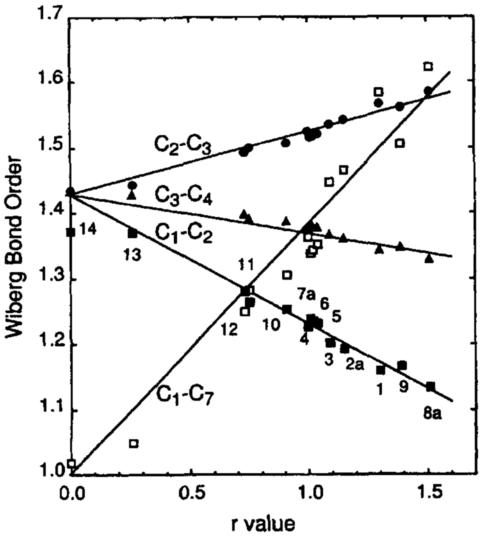

Figure 10. Wiberg bond orders from NBO analysis (RHF/6-31G*) vs *r* values for benzylic cations. Numbers as in Figure 1

Bond length vs *r* value

For a series of benzylic cations, the C_1—C_7 bond length and the lengths of the C_1—C_2 (or C_6—C_1), C_2—C_3 (or C_5—C_6) and C_3—C_4 (or C_4—C_5) bonds optimized at the RHF/6-31G* level (in Tables 2–5) exhibit characteristic changes, in line with the varying degree of resonance interaction between the benzylic pπ orbital and the benzene π system. The 'resonance theory' predicts elongation of C_1—C_2 and C_3—C_4 and shortening of C_1—C_7 and C_2—C_3 with increasing degree of conjugation. The C_1—C_7, C_1—C_2, C_2—C_3 and C_3—C_4 bond lengths at the RHF/6-31G* level are plotted against the *r* values in Figures 11 and 12. There is a linear correlation

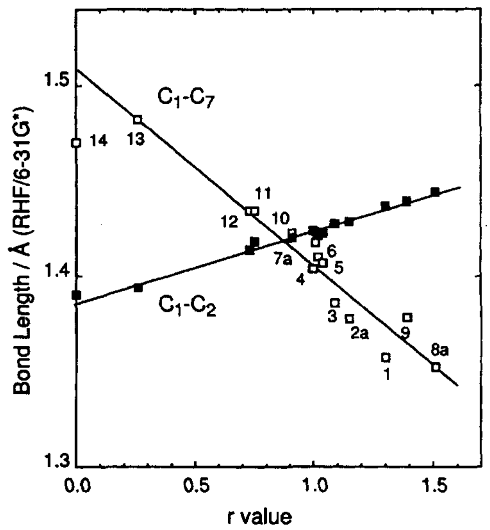

Figure 11. Bond length vs *r* value for benzylic cations. Numbers as in Figure 1

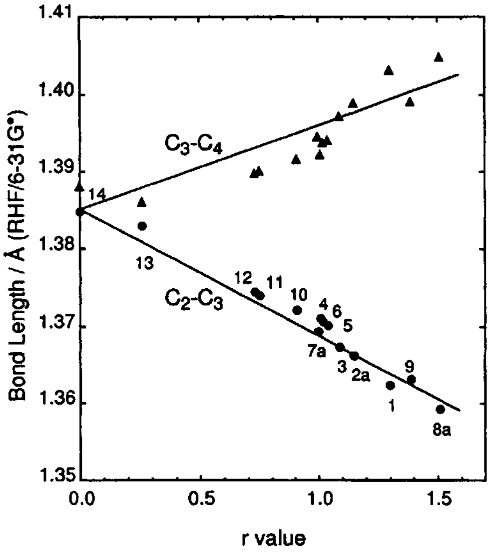

Figure 12. Bond length vs *r* value for benzylic cations. Numbers as in Figure 1

with the *r* value for C_1—C_7 ($R = 0{\cdot}96$) and for the lengths of the respective benzene C—C bonds ($R = 0{\cdot}98$). The C_1—C_7 bond length decreases significantly with increased resonance demand (Figure 11). The C_1—C_7 bond length at $r = 0$ is estimated to be 1·52 Å, which is close to the normal carbon–carbon single bond length (1·53 Å in ethane[7] and 1·517 Å from equation (7)), whereas at $r = 1{\cdot}5$ the C_1—C_7 bond length is 1·35 Å, which is close to the normal carbon–carbon double bond length (1·32 Å in ethylene[7]). The bond lengths of the aromatic ring are estimated to be 1·39 Å at $r = 0$, which is close to the carbon–carbon bond length of benzene.[7] As the *r* value increases, the C_1—C_2 (Figure 11) and C_3—C_4 (Figure 12) bonds are lengthened, but the C_2—C_3 bond (Figure 12) is shortened. The C_1—C_2 bond length shows a higher susceptibility to the *r* value than does the C_3—C_4 bond length. This is in line with the prediction of the resonance theory. Assuming equivalent contributions of the five resonance structures shown in Figure 7, C_1—C_7 and C_2—C_3 decrease but C_1—C_2 and C_3—C_4 increase, keeping C_1—$C_2 > C_3$—C_4, compared with the localized structures (I and V). As a result, all these plots are correlated linearly following the resonance theory. As mentioned above, the behaviour of *r* is completely consistent with what is envisaged for the resonance demand, and also the resonance interaction between C_7 and the aromatic moiety changes in parallel with the *r* value.

The empirical *r* values in the YT substituent effect analysis are well correlated with all calculated indices (charge distribution, bond order and bond length) for benzylic cations. The relationship between each theoretical index and the *r* value agreed completely with the prediction of the resonance theory. This provides theoretical support to the contention that the *r* value is a good parameter indicating the degree of resonance interaction between the benzylic pπ orbital and the benzene π system.

ACKNOWLEDGEMENTS

This work was supported by a Grand-in-Aid for Developmental Scientific Research from the Ministry of Education, Science and Culture, Japan.

REFERENCES

1. J. Shorter, in *Correlation Analysis in Chemistry*, edited by N. B. Chapman and J. Shorter, pp. 11973. Plenum Press, New York (1978).
2. L. P. Hammett, *Physical Organic Chemistry*, Chapt. VII. McGraw-Hill, New York (1940).
3. H. C. Brown and Y. Okamoto, *J. Am. Chem. Soc.* **79**, 1913–1917 (1957).
4. (a) A. Murata, M. Goto, R. Fujiyama, M. Mishima, M. Fujio and Y. Tsuno, *Bull. Chem. Soc. Jpn.* **63**, 1129–1137 (1990); (b) A. Murata, S. Sakaguchi, R. Fujiyama, M. Fujio and Y. Tsuno, *Bull. Chem. Soc. Jpn.* **63**, 1138–1145 (1990); (c) M. Fujio, M. Goto, T. Susuki, I. Akasaka, M. Mishima and Y. Tsuno, *Bull. Chem. Soc. Jpn.* **63**, 1146–1153 (1990); M. Fujio, M. Goto, T. Susuki, M. Mishima,and Y. Tsuno, *J. Phys. Org. Chem.* **3**, 449–455 (1990); (d) Y. Tsuno, Y. Kusuyama, M. Sawada, T. Fujii and Y. Yukawa, *Bull. Chem. Soc. Jpn.* **48**, 3337–3346 (1975); M. Fujio, T. Adachi, Y. Shibuya, A. Murata and Y. Tsuno, *Tetrahedron Lett.* **25**, 4557–4560 (1984); (e) Y. Tsuji, M. Fujio and Y. Tsuno, *Bull. Chem. Soc. Jpn.* **63**, 856–866 (1990); (f) M. Fujio, Y. Tsuji, T. Otsu and Y. Tsuno, *Tetrahedron Lett.* **32**, 1805–1808 (1991); (g) M. Fujio, K. Nakata, Y. Tsuji, T. Otsu and Y. Tsuno, *Tetrahedron Lett.* **33**, 321–324 (1992); (h) M. Fujio, K. Nakata, T. Kuwamura, H. Nakamura, Y. Saeki, M. Mishima, S. Kobayashi and Y. Tsuno, *Tetrahedron Lett.* **34**, 8309–8312 (1993); (i) M. Fujio, H. Nomura, K. Nakata, Y. Saeki, M. Mishima, S. Kobayashi, T. Matsushita, K. Nishimoto and Y. Tsuno, *Tetrahedron Lett.* **35**, 5005–5008 (1994); (i) M. Fujio, T. Miyamoto, Y. Tsuji and Y. Tsuno, *Tetrahedron Lett.* **32**, 2929–2932 (1991); (k) M. Fujio, K. Nakashima, E. Tokunaga, Y. Tsuji and Y. Tsuno, *Tetrahedron Lett.* **33**, 345–348 (1992).
5. Y. Yukawa and Y. Tsuno, *Bull. Chem. Soc. Jpn.* **32**, 971–981 (1959); Y. Yukawa, Y. Tsuno and M. Sawada, *Bull. Chem. Soc. Jpn.* **39**, 2274–2286 (1966).
6. (a) M. Mishima, H. Inoue, M. Fujio and Y. Tsuno, *Tetrahedron Lett.* **30**, 2101–2104 (1989); (b) M. Mishima, H. Inoue, M. Fujio and Y. Tsuno, *Tetrahedron Lett.* **31**, 685–688 (1990); (c) M. Mishima, K. Arima, S. Usui, M. Fujio and Y. Tsuno, *Mem. Fac. Sci. Kyushu Univ., Ser. C* **15**, 277–286 (1986); M. Mishima, K. Arima, S. Usui, M. Fujio and Y. Tsuno, *Chem. Lett.* 1047–1050 (1987); (d) M. Mishima, S. Usui, M. Fujio and Y. Tsuno, *Nippon Kagaku Kaishi* 1269–1274 (1989); (e) M.

Mishima, H. Nakamura, K. Nakata, M. Fujio and Y. Tsuno, *Chem. Lett.* 1607–1610 (1994); (f) M. Mishima, S. Usui, H. Inoue, M. Fujio and Y. Tsuno, *Nippon Kagaku Kaishi* 1262–1268 (1989); (g) M. Mishima, K. Nakata, H. Nomura, M. Fujio and Y. Tsuno, *Chem. Lett.* 2435–2438 (1992); K. Nakata, H. Nomura, M. Mishima, Y. Saeki, K. Nishimoto, T. Matsushita, M. Fujio and Y. Tsuno, *Mem. Fac. Sci. Kyushu Univ., Ser. C* **18**, 287–296 (1992).

7. W. J. Hehre, L. Radom, P. v. R. Schleyer and J. A. Pople, *Ab initio Molecular Orbital Theory.* Wiley, New York (1986).
8. M. J. Frisch, G. W. Trucks, M. Head-Gordon, P. M. W. Gill, M. W. Wong, J. B. Foresman, B. G. Johnson, H. B. Schlegel, M. A. Robb, E. S. Replogle, R. Gemperts, J. L. Andres, K. Raghavachari, J. S. Binkley, C. Gonzalez, R. L. Martin, D. J. Fox, D. J. DeFrees, J. Baker, J. J. P. Stewart and J. A. Pople, *Gaussian 92*. Gaussian, Pittsburgh, PA (1992).
9. C. Møller and M. S. Plesset, *Phys. Rev.* **46**, 618–622 (1934).
10. J. A. Pople, H. B. Schlegel, R. Krishnan, D. J. DeFrees, J. S. Binkley, M. J. Frisch, R. A. Whiteside, R. F. Hout and W. J. Hehre, *Int. J. Quantum Chem., Quantum Chem. Symp.* **15**, 269–278 (1981); D. J. DeFrees and A. D. McLean, *J. Chem. Phys.* **82**, 333–341 (1985).
11. R. S. Mulliken, *J. Chem. Phys.* **23**, 1833–1840 (1955).
12. A. E. Reed, R. B. Weinstock and F. Weinhold, *J. Chem. Phys.* **83**, 735–748 (1985); A. E. Reed, L. A. Curtiss and F. Weinhold, *Chem. Rev.* **88**, 899–926 (1988); J. E. Carpenter and F. J. Weinhold, *J. Mol. Struct.* **169**, 41–62 (1988).
13. W. J. Hehre, M. Taagepera, R. W. Taft and R. D. Topsom, *J. Am. Chem. Soc.* **103**, 1344–1349 (1981).
14. A. E. Dorigo, Y. Li and K. N. Houk, *J. Am. Chem. Soc.* **111**, 6942–6948 (1989).
15. K. Raghavachari, R. A. Whiteside, J. A. Pople and P. v. R. Schleyer, *J. Am. Chem. Soc.* **103**, 5649–5657 (1981).
16. P. v. R. Schleyer and J. W. de M. Carneiro, *J. Am. Chem. Soc.* **113**, 3990–3992 (1991).
17. S. Sieber, P. Buzek, P. v. R. Schleyer, W. Koch and J. W. de M. Carneiro, *J. Am. Chem. Soc.* **115**, 259–270 (1993).
18. R. B. Woodward and R. Hoffmann, *J. Am. Chem. Soc.* **87**, 395–397 (1965).
19. K. Nishimoto and L. S. Forster, *Theor. Chim. Acta* **3**, 407–417 (1965).
20. K. B. Wiberg, *Tetrahedron* **24**, 1083–1096 (1968).